remote sensing

MDPI

Article

Spatio-Temporal Monitoring of the Invasive Plant *Alternanthera philoxeroides* in a Narrow River Using Sentinel-2 Time-Series Data

Kengo Shinohara * and Hideharu Kurita

Institute for Rural Engineering, National Agriculture and Food Research Organization (NARO), Tsukuba 305-8609, Japan
* Correspondence: shinohara.kengo338@naro.go.jp; Tel.: +81-29-838-7555

Highlights

What are the main findings?

- A multi-temporal Sentinel-2 data approach was applied for the first time to analyze and visualize the spatiotemporal dynamics of fractional vegetation cover (FVC) for *Alternanthera philoxeroides* in the Hachiken River, Chiba, Japan, estimating FVC with an RMSE of 8.5% even in a narrow (~24 m) river channel.
- Multi-temporal analysis (2019–2024) detected a downstream expansion starting in 2022 and demonstrated that the suppression effect of removal activities on the annual maximum cover C_{max} persisted for only about one year.

What are the implications of the main findings?

- The satellite-based FVC visualization approach validated in the Hachiken River enables consistent and continuous monitoring of invasive plant dynamics across entire river systems.
- Structural factors (bank type) and management factors (removal activities) can be quantitatively compared and evaluated using time-series data, thereby supporting evidence-based invasive alien species (IAS) control planning.

Abstract

Alternanthera philoxeroides, an invasive alien species, spreads rapidly in river systems via vegetative propagation from stem fragments, requiring river-system-scale monitoring to understand its expansion dynamics and habitat preferences. This study used multi-temporal Sentinel-2 data to analyze spatio-temporal variations in fractional vegetation cover (FVC) within a 3.5 km river reach. FVC estimates derived from vegetation indices were validated against high-resolution aerial images, with an EVI-based model achieving the highest accuracy (RMSE = 9.2%), enabling reliable monitoring even in narrow (~24 m) channels. Time-series analysis from 2019 to 2024 revealed downstream expansion beginning in 2022. Annual maximum FVC (C_{max}) was used to assess relationships with removal records and bank structures, showing that removal effects were temporary and more pronounced in the first year, while steel sheet-pile banks limited vegetation growth compared to concrete revetments. These results demonstrate that Sentinel-2 data can provide an effective and accessible tool for evaluating invasive plant dynamics and management effectiveness in low-flow river systems where *A. philoxeroides* dominates the floating vegetation community.

Keywords: invasive alien species; Sentinel-2 satellite data; time series analysis

Check for updates

Academic Editor: Sandra Eckert

Received: 1 June 2026
Revised: 18 July 2026
Accepted: 20 July 2026
Published: 27 July 2026

1. Introduction

Among biological species introduced from outside into specific regions or ecosystems, those that cause severe impacts on native species, ecosystems, or human activities are defined as invasive alien species (IAS) [1,2]. IAS are widely recognized as one of the major drivers of biodiversity loss and species extinction worldwide [3]. Furthermore, the importance of addressing IAS for biodiversity conservation is explicitly recognized in the Strategic Plan for Biodiversity 2011–2020 and the Aichi Biodiversity Targets adopted at the 10th Conference of the Parties to the Convention on Biological Diversity (COP10) [4].

In recent years, *Alternanthera philoxeroides* (Mart.) Griseb. has emerged as a prominent IAS characterized by expanding invasive ranges and increasing damage. This species grows vigorously in paddy fields and adjacent rivers, causing ecological disturbances, competition with crops [5], and issues related to flood control and water use, such as the obstruction of agricultural drainage [6]. Moreover, it forms mat-like colonies that cover the water surface, inhibiting light penetration and gas exchange and thereby exerting negative impacts on aquatic environments [7]. Native to South America, it has extensively invaded North America, Australia, New Zealand, Southeast Asia, India, and China [8]. In Japan, its invasion and establishment were first confirmed in 1989, and as of 2025, its distribution had expanded to 31 prefectures [9].

Several studies on IAS emphasize that understanding when, where, and to what extent a target species proliferates is crucial for formulating management plans and selecting priority reaches. For instance, Kim et al. pointed out that understanding the intrinsic rate of increase of an invasive species is critical for determining budget allocations between prevention and removal [10]. Mehta et al. viewed colony detection as an investment process that determines subsequent removal costs and evaluated factors such as detectability, survey effort, and population density [11]. Ramula compared the population growth rates of 21 invasive and 179 native plant species by indexing survival, growth, and fecundity, and argued that effective management can be achieved only by simultaneously targeting multiple processes, such as "survival + growth" [12]. Furthermore, Santos et al. reported that the growth patterns of Egeria densa significantly reduce the species richness and biomass of native species in large-scale aquatic systems and argued that rapid assessments that consider seasonality are indispensable for effective management [13].

River environments, in particular, play a vital role in the invasion, establishment, and dispersal of invasive plants. Rivers are dynamic and continuous environments extending from upstream to downstream, where plant fragments can travel long distances and establish following disturbances such as floods, leading to new invasions or re-infestations. Such environmental changes have been reported to facilitate the establishment of invasive plants and the exclusion of native species [14], and invasive plants have also been described as "ecosystem engineers" because they alter sedimentation and flow velocity, thereby affecting the physical and ecological environment of the entire river channel [13]. Consequently, understanding spatio-temporal proliferation dynamics at the river-system scale—which is difficult to capture through local observations alone—is important for effective management.

However, wide-area monitoring aimed at capturing spatio-temporal dynamics of *A. philoxeroides* at a river-system scale remains limited. Most previous studies have focused on individual colony management in specific lakes or ponds [6] or on visualizing distribution using single-period aerial photographs [15]. In analyses using satellite data, broad-scale sensors such as MODIS lack the spatial resolution required to capture linear distributions in small- to medium-sized rivers [16]. Conversely, studies using high-resolution sensors tend to be limited in analytical scope or restricted to single-year or single-period evaluations due to cost and data acquisition frequency constraints [17,18]. Although Clements et al. [19]

quantified the expansion process of coverage area over time using satellite data, their study focused on lentic environments (lakes) and did not track wide-area dynamics in flowing river environments. Thus, there remains insufficient research that systematically organizes and compares observed colony-scale reach conditions over time at a river-system scale.

Therefore, the primary objective of this study was to develop and demonstrate a Sentinel-2-based framework for monitoring the spatio-temporal dynamics of *A. philoxeroides* in a narrow river system. Using the developed FVC estimation model and time-series analysis framework, we further explored how removal activities and revetment structures were associated with observed vegetation dynamics as practical applications of the proposed monitoring approach.

2. Materials and Methods

Figure 1 illustrates the overall workflow of the study. First, a conversion model for fractional vegetation cover (FVC) was developed by comparing reference FVC values derived from visual interpretation of high-resolution Google aerial photographs with vegetation indices (NDVI, EVI, and MSAVI) obtained from Sentinel-2 imagery. The resulting model was then applied to Sentinel-2 time-series data from 2019 to 2024 to estimate spatio-temporal variation in FVC across the entire river. Subsequently, annual maximum fractional vegetation cover (C_{max}) was derived for each segment and used to evaluate infestation dynamics in relation to removal records and revetment structures.

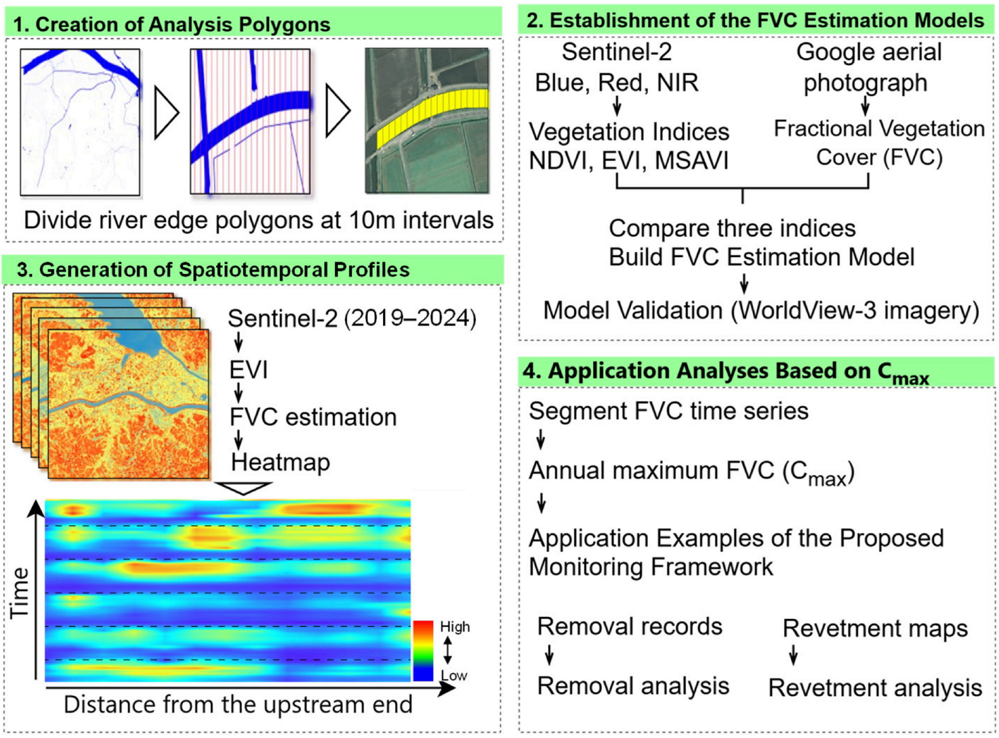

Figure 1. Workflow of satellite data analysis.

2.1. Study Area and Target Species

In this study, we analyzed the distribution and temporal changes in *A. philoxeroides* colonies using multi-temporal Sentinel-2 satellite data, focusing on the downstream reach of the Hachiken River (approximately 24 m wide and 3.5 km long) located in Katori City, Chiba Prefecture, Japan (Figure 2), following the workflow shown in Figure 1.

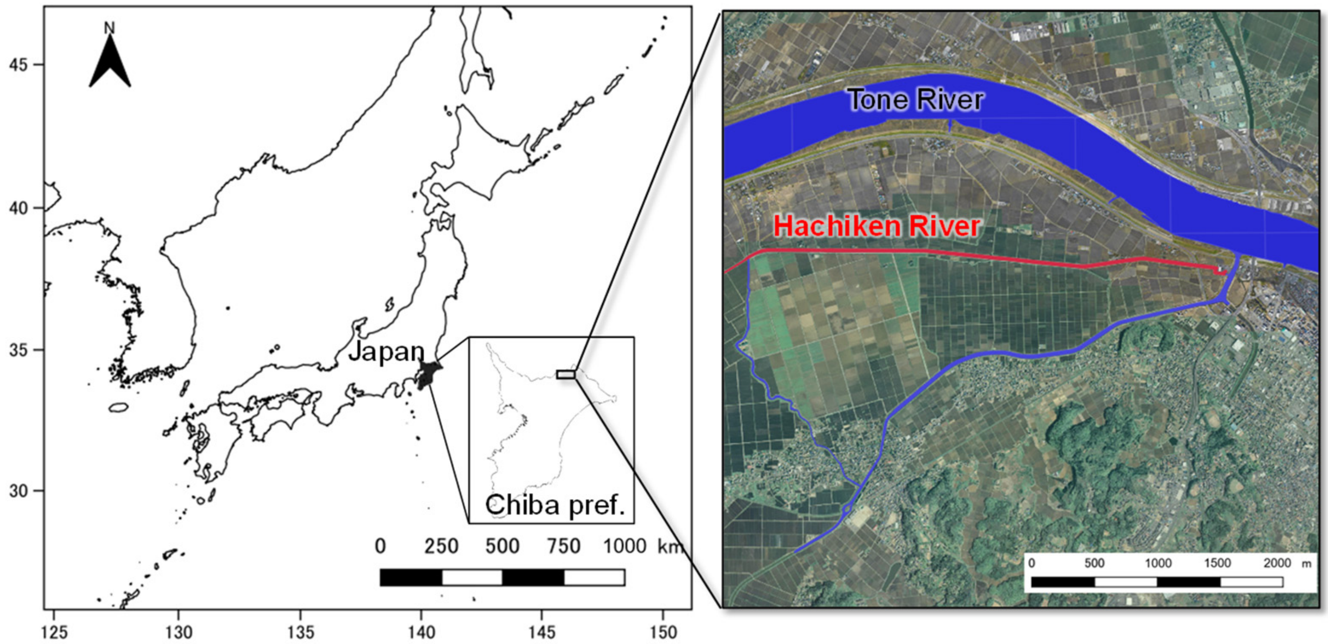

Figure 2. Location of the study area.

The Hachiken River has a total length of 7.3 km and is characterized by extremely low flow velocities throughout the channel; depending on the operational status of the pumping stations, gentle backflow may occur. A junction with a distributary is located 3.8 km from the upstream end, and the proliferation of *A. philoxeroides* has been confirmed in the reach downstream of this point (a 3.5 km stretch). Although regular removal operations are conducted by river managers to prevent flow obstructions and other issues, the species rapidly re-infests the area, making it difficult for removal efforts to keep pace with its growth.

Furthermore, this species is known to outcompete neighboring native plants and tends to form monospecific stands [19–21]. Field observations conducted throughout the study reach in August 2024 and November 2024, together with the interpretation of high-resolution aerial imagery, confirmed that the vast majority of floating vegetation covering the water surface within the study reach consisted of *A. philoxeroides*. Other aquatic plant species were observed only locally and did not represent a substantial proportion of the total vegetation cover. Therefore, vegetation cover estimated in this study was used as a proxy for the extent of *A. philoxeroides* colonies. For convenience, the study reach was divided into segments numbered St. 1 to St. 13 at 240 m intervals from the upstream end.

2.2. Sentinel-2 Satellite Data

Sentinel-2 is a constellation of Earth observation satellites operated by the European Space Agency (ESA) that provides data free of charge. Although its spatial resolution is relatively coarse (10 m), its high observation frequency (5-day revisit time) makes it a suitable data source for continuous environmental monitoring at a river-system scale. For this study, Sentinel-2A and Sentinel-2B Level-2A products covering the Hachiken River basin in Katori City, Chiba Prefecture, were obtained from the Copernicus Browser website (https://browser.dataspace.copernicus.eu). Scenes captured under clear-sky conditions between 2019 and 2024 were selected at a frequency of approximately one scene per month for each year.

For each acquired scene, the positional relationship with the waterline and the river channel geometry was verified using aerial photographs provided by the Geospatial Information Authority of Japan (GSI) as reference data. The positional relationship between the river channel and surrounding features was visually inspected for all Sentinel-2 scenes. This verification revealed positional offsets of several meters in some images across the time series. Geometric correction was therefore applied only to scenes showing obvious spatial misalignment. Correction was performed using the Georeferencer tool in QGIS (ver. 3.34.8) with a Helmert transformation based on three ground control points (GCPs) located at road intersections. After correction, the consistency of river-channel geometry and shoreline positions among the time-series images was visually confirmed before further analysis.

The number of usable Sentinel-2 scenes was 13, 13, 13, 14, 14, and 10 for 2019, 2020, 2021, 2022, 2023, and 2024, respectively, indicating relatively similar observation frequencies among years.

2.3. Development of an FVC Estimation Model

To appropriately estimate the FVC of *A. philoxeroides* colonies using Sentinel-2 data, we first conducted a comparative evaluation of multiple vegetation indices. In this study, FVC was used as an indicator of the spatial extent and temporal dynamics of *A. philoxeroides* colonies. Reference FVC values represent the proportion (%) of vegetation cover within each water-segment polygon and were derived through the interpretation of high-resolution aerial photographs. This species forms mat-like colonies on the water surface and possesses spectral characteristics similar to those of common aquatic plants, exhibiting strong reflectance in the near-infrared region and weak reflectance in the red region. The relationship between FVC and spectral reflectance is considered relatively clear for this species because it tends to form dense, monospecific stands [22]. However, research on the quantitative estimation of FVC for this species using satellite remote sensing remains limited. In particular, few studies have reported direct estimations of FVC in narrow rivers using Sentinel-2 data; most previous studies have been limited to presence/absence classification or area extraction using aerial photographs or high-resolution satellite imagery [19,22].

Therefore, this study evaluated three indices commonly used in IAS monitoring—the Normalized Difference Vegetation Index (NDVI), the Enhanced Vegetation Index (EVI), and the Modified Soil Adjusted Vegetation Index (MSAVI)—to determine which index is most suitable for estimating the FVC of *A. philoxeroides* using Sentinel-2 data. NDVI is the most widely used fundamental index. EVI has been reported to be effective for evaluating aquatic vegetation because it accounts for atmospheric and water-surface effects [23]. MSAVI is designed to minimize soil background noise under sparse vegetation conditions. In invasive plant research, MSAVI has been employed to accurately capture low-coverage populations during the initial invasion stage or sparse colonies during seasonal decline [24].

$$\mathrm{NDVI} = \frac{\mathrm{NIR} - \mathrm{Red}}{\mathrm{NIR} + \mathrm{Red}} \tag{1}$$

$$\mathrm{EVI} = \mathrm{G} \times \frac{\mathrm{NIR} - \mathrm{Red}}{\mathrm{NIR} + \mathrm{C_1} \times \mathrm{Red} - \mathrm{C_2} \times \mathrm{Blue} + \mathrm{L}} \tag{2}$$

$$\mathrm{MSAVI} = \frac{2 \times \mathrm{NIR} + 1 - \sqrt{(2 \times \mathrm{NIR} + 1)^2 - 8 \times (\mathrm{NIR} - \mathrm{Red})}}{2} \tag{3}$$

Here, NIR, Red, and Blue represent the pixel values (reflectance) of the near-infrared, red, and blue bands, respectively, while G, C_1, C_2, and L are constants. Based on Huete et al. [23], G, C_1, C_2, and L were set to 2.5, 6, 7.5, and 1, respectively. For the Blue, Red, and NIR bands, pixel values from Bands 2, 4, and 8 of the Sentinel-2 data were used.

Next, river polygons created by dividing the river area into 10 m intervals in the east–west direction based on waterline data (hereafter referred to as "water-segment polygons") were overlaid on each image. The mean pixel values within each polygon (hereafter referred to as "segment-mean NDVI," "segment-mean EVI," and "segment-mean MSAVI") were then calculated.

In general, vegetation indices are influenced by the physiological state of plants associated with growth stages and seasonal changes. Particularly after the peak growth period, the relationship between these indices and vegetation cover may become non-linear because of changes in leaf color and spectral characteristics. Regarding this point, Verschoren et al. [25] noted in a study on riverine vegetation that seasonal lighting conditions and plant life history can affect coverage evaluation through image analysis. Furthermore, Liu et al. [26] demonstrated that, in large-scale, long-term analyses, using an NDVI-based dimidiate pixel model can reduce uncertainties arising from the spectral characteristics of non-vegetated areas, enabling stable vegetation cover estimation even under conditions involving seasonal variation.

Therefore, rather than relying on data from a single period, this study constructed a conversion model by integrating data from multiple periods representing different growth stages and spectral characteristics. Using all available Google aerial photographs acquired during the observation period (16 May 2018; 8 May 2019; 20 February 2021; 5 December 2021; 25 November 2022; and 30 November 2023), the FVC ratio relative to the area of the water-segment polygons (hereafter referred to as "segment-mean FVC"; 0–100%) was calculated by manually tracing colony outlines. Colony tracing followed the method of Clements et al. (2011) [19], who performed similar work, and all tracing was conducted by the same analyst. The validity of the image interpretation results was confirmed by comparing colony shapes identified in aerial photographs with those in ground-level photographs available on Google Street View.

Next, a scatter plot was created using the determined segment-mean FVC and the segment-mean NDVI, EVI, and MSAVI values calculated from Sentinel-2 data acquired at approximately the same time (15 May 2018; 8 May 2019; 21 February 2021; 5 December 2021; 25 November 2022; and 30 November 2023). An FVC conversion formula was then constructed by fitting a linear regression equation to each plot. Data from five of the six periods for which aerial photographs were obtained were used to build the conversion model, whereas the remaining period (30 November 2023) was reserved as independent validation data. For the FVC conversion formulas constructed for each vegetation index, the correlation coefficient (r) between the segment-mean vegetation index values and segment-mean FVC was calculated using the training data (five periods). Additionally, the root mean square error (RMSE), based on the difference between estimated FVC and reference FVC, was calculated as an evaluation metric. Furthermore, the generalization performance of each conversion model was evaluated by applying each formula to the independent validation data and calculating the RMSE between the estimated FVC and segment-mean FVC obtained from Google aerial photographs.

The visual interpretation of Google aerial photographs and tracing of colony outlines were conducted for the reach (110 m to 720 m from the upstream end) where colony shapes were clearly identifiable across all six analysis periods. This calibration reach was divided into 61 water-segment polygons at 10 m intervals. Five observation dates were used for model calibration, resulting in 305 calibration observations (61 polygons $\times$ 5 dates), while the remaining observation date was reserved for independent validation, resulting in 61 validation observations. In addition, leave-one-date-out cross-validation (LODO-CV) using all six reference dates was conducted to further evaluate model robustness.

2.4. Evaluation of Colony Formation Characteristics Using Maximum FVC C_{max}

From a river management perspective, it is important to understand not only the fluctuating process of FVC but also the vegetation coverage state during the peak growth season, when impacts on flow capacity and the ecosystem are maximized. Clements et al. [19] evaluated maximum summer growth through time-series analysis of aerial photographs. In this study, we used temporal changes in FVC estimated from Sentinel-2 data to understand seasonal fluctuations and extracted the annual maximum fractional vegetation cover (C_{max}; 0–100%) observed each year as an index for evaluating the colony formation characteristics of this species. Annual maximum fractional vegetation cover (C_{max}) was calculated exclusively from FVC values derived from actual Sentinel-2 observation dates and was not derived from interpolated values. The spatio-temporal Kriging procedure was used solely for the visualization of broad-scale patterns. Furthermore, by comparing the calculated FVC and C_{max} with removal records (timing and location) obtained from river managers and revetment construction plans, we discussed the inhibitory effects of removal on colony formation and differences in proliferation characteristics among different revetment types in the Hachiken River.

The maximum FVC C_{max} defined in this study is an index representing the maximum coverage state reached by *A. philoxeroides* colonies each year. It is intended to represent the state during the peak season—which has the greatest management impact—among seasonally varying vegetation coverage levels. This index indicates the upper limit of colony extent actually reached under field conditions influenced by river channel conditions, revetment structures, and removal events; it does not directly correspond to carrying capacity in the mathematical biological sense [27], in which such conditions are excluded. However, because this study uses vegetation coverage for wide-area, long-term monitoring, C_{max} is positioned as a proxy for carrying capacity, representing the colony extent realized under specific environmental and management conditions.

Spatially referenced removal records provided by the river manager were obtained from river managers in CAD format and imported into QGIS for analysis. Specifically, revetment design plans and time-series records of removal activities were converted from CAD format into vector layers and integrated with the water-segment polygons to identify the timing of removal in each river segment.

To facilitate visualization of the spatio-temporal dynamics of vegetation cover, segment-based FVC values were interpolated using the spatio-temporal Kriging function implemented in Surfer 23.2.176 (Golden Software, LLC., Golden, CO, USA). A linear variogram model was adopted with no trend removal. Interpolation was performed using a spatial grid size of 10 m, corresponding to the original Sentinel-2 spatial resolution, and a temporal resolution of one day. The input dataset consisted of segment-based FVC observations derived from individual Sentinel-2 acquisition dates. Spatial and temporal gaps between observation points were estimated using spatio-temporal Kriging to generate continuous visualization surfaces.

3. Results and Discussion

3.1. Development of the FVC Estimation Model

By comparing the FVC of *A. philoxeroides* calculated from Google aerial photographs with the segment-mean NDVI, EVI, and MSAVI values, we constructed FVC conversion formulas for each vegetation index and evaluated their estimation accuracy.

The results indicated that EVI achieved the highest predictive accuracy among the three vegetation indices based on both training-data performance and leave-one-date-out cross-validation results (Figure 3, Table 1).

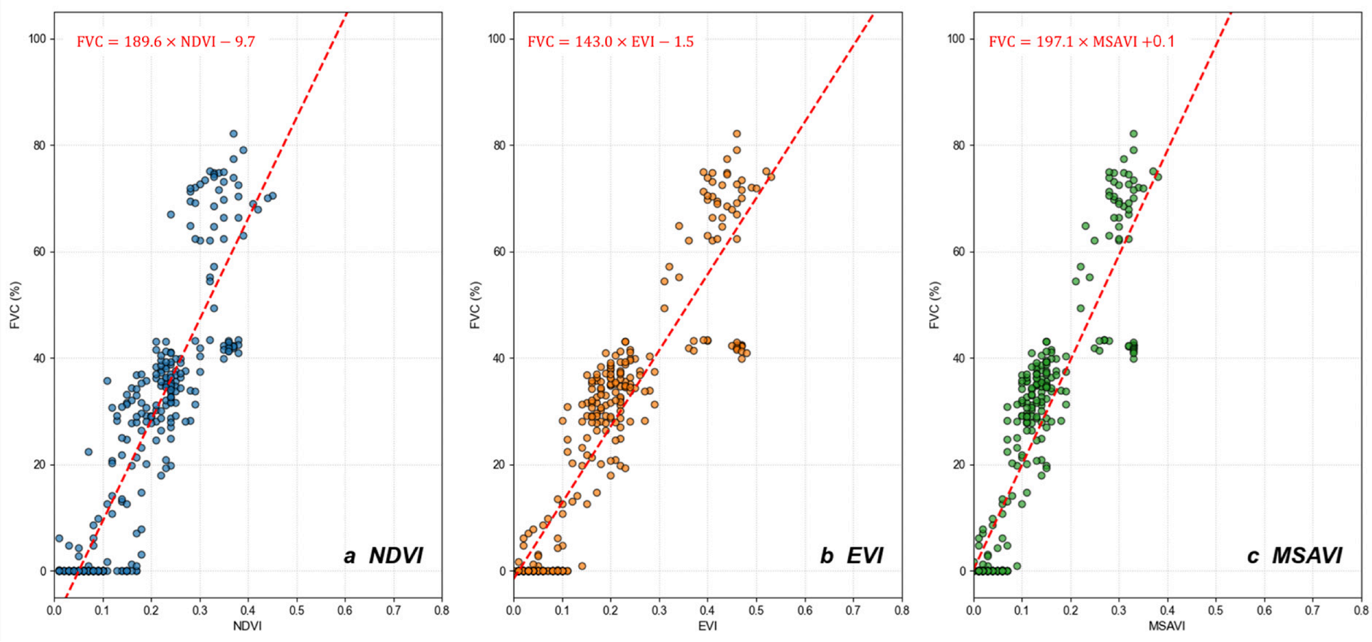

Figure 3. Relationships between segment-mean NDVI (**a**), EVI (**b**), and MSAVI (**c**) values derived from Sentinel-2 satellite data and segment-mean FVC determined by tracing Google aerial photographs.

Table 1. Coverage–index conversion models and their accuracy.

Vegetation Index	Model	r (Training Data)	RMSE (Training Data, %)	Mean RMSE (Leave-One-Date-Out CV, %)
NDVI	FVC = 189.6 × NDVI − 9.7	0.899	10.4	10.0
EVI	FVC = 143.0 × EVI − 1.5	0.923	9.2	9.2
MSAVI	FVC = 197.1 × MSAVI + 0.1	0.919	9.4	10.0

To further evaluate model robustness, leave-one-date-out cross-validation (LODO-CV) was conducted using the six available reference dates. The mean RMSE values obtained from LODO-CV were 10.0%, 9.2%, and 10.0% for NDVI, EVI, and MSAVI, respectively (Table 1). For the selected EVI model, RMSE values ranged from 3.9% to 14.5% across the six validation iterations. EVI consistently showed the lowest prediction error and was therefore selected for subsequent analyses.

Although MSAVI is an index capable of reducing the influence of soil background reflectance under sparse vegetation conditions, the water-segment polygons in this study area contained only the water surface and *A. philoxeroides* colonies, with virtually no exposed soil surfaces. Therefore, the effect of soil noise reduction expected from MSAVI was likely limited. In contrast, EVI utilizes the Blue band, allowing correction for the effects of atmospheric aerosol scattering and water-surface reflectance. This characteristic is considered to have contributed to the higher estimation accuracy of the EVI model.

The study river has a width of approximately 24 m, meaning that Sentinel-2 data with a spatial resolution of 10 m are inevitably subject to mixed-pixel (mixel) effects, in which water and riverbank areas coexist within a single pixel. Particularly when colonies are formed predominantly along the banks, segment-mean FVC may be underestimated or overestimated due to mixing with background reflectance (e.g., bank vegetation or revetment structures), even when the actual coverage is high [17]. This factor may have contributed to the reduced estimation accuracy of the models.

Furthermore, it should be noted that the reference FVC values in this study were calculated through visual interpretation of high-resolution Google aerial photographs, which inherently includes uncertainties arising from analyst subjectivity, as well as differences in solar altitude and water surface reflection conditions at the time of capture.

Consequently, although these multiple sources of error should be considered, we confirmed that the FVC estimation model using EVI achieved relatively high accuracy and therefore adopted this model for subsequent analyses. This study prioritizes analytical consistency by conducting all time-series assessments at the same spatial resolution (Sentinel-2, 10 m) and identical methodology. Therefore, care should be taken to interpret the obtained FVC and C_{max} values not as strict representations of localized actual coverage rates but rather as relative indicators for comparing colony extent across different segments and years.

The EVI–FVC model developed in this study was intentionally calibrated using observations acquired under multiple seasonal conditions, including spring, winter, and late autumn, to establish a generalized relationship applicable to long-term monitoring. The model showed a positive relationship between EVI and reference FVC in the calibration dataset (r = 0.923).

Furthermore, vegetation cover interpreted from WorldView-3 imagery was compared with Sentinel-2-derived FVC estimates across the entire study reach to evaluate spatial transferability beyond the calibration area. A positive relationship was observed (r = 0.909), indicating that the model captured the major spatial variability in vegetation cover throughout the river. Collectively, these results support the applicability of the proposed model for monitoring vegetation-cover dynamics within the study river.

Nevertheless, uncertainties associated with seasonal variability, riverbank conditions, background reflectance characteristics, mixed-pixel effects, and the limited number of reference observation dates remain. Additional validation under a wider range of environmental conditions would further strengthen confidence in the robustness and transferability of the approach.

The reference FVC values were derived from manual interpretation of high-resolution Google aerial photographs and therefore inevitably contain uncertainty associated with image interpretation. Potential error sources include subjective delineation of colony boundaries, shadow effects, water-surface reflection, and ambiguity in partially vegetated areas. Because these interpreted FVC values were subsequently used for calibration of the EVI–FVC model, such uncertainties may propagate into both the regression model and the resulting FVC estimates. Although Google Street View images were used for supplementary visual confirmation, they do not constitute a systematic field validation. Therefore, the FVC values presented in this study should be interpreted primarily as indicators of relative spatial and temporal variation rather than exact measures of absolute vegetation cover.

The proposed framework does not directly detect *A. philoxeroides* from its spectral characteristics. Rather, it estimates the fractional vegetation cover of floating or surface-covering vegetation within the river channel. Field observations and aerial-image interpretation indicated that the vast majority of surface-covering vegetation in the study reach consisted of *A. philoxeroides*, allowing vegetation cover to be used as a proxy for the extent of *A. philoxeroides* colonies. However, in river systems where multiple aquatic plant species coexist or species composition changes substantially over time, the estimated FVC may not correspond directly to the cover of *A. philoxeroides*. Therefore, application of the proposed method is most appropriate in systems where this species is known to dominate the floating vegetation community.

3.2. Spatio-Temporal Variations in FVC

By applying the EVI–FVC equation developed in the previous section to the Sentinel-2 dataset, we calculated segment-mean FVC for each location and observation date. To intuitively capture the spatio-temporal trends in vegetation coverage distribution across the entire river, the obtained FVC values were interpolated using the spatio-temporal Kriging method in Surfer 23.2.176 (Golden Software, LLC.). This enabled the generation of an FVC heatmap, in which the vertical axis represents time (1 January 2019 to 31 December 2024) and the horizontal axis represents distance from the upstream end (Figure 4).

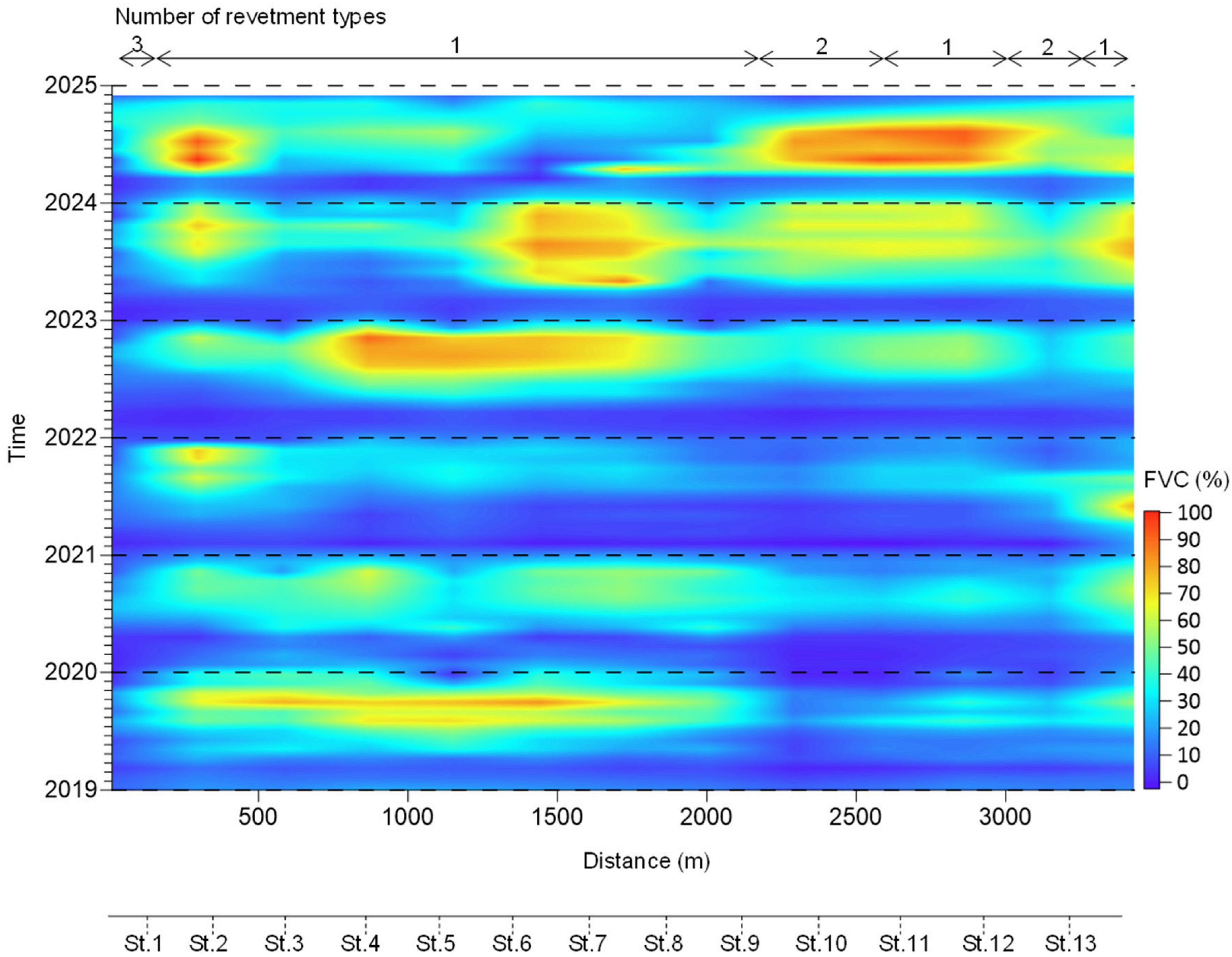

Figure 4. Spatio-temporal heatmap of segment-averaged vegetation coverage.

Focusing first on the chronological changes across the entire river, the maximum FVC remained around 80% from 2019 to 2021, indicating that infested areas were limited. Conversely, from 2022 onward, the FVC reached nearly 100% at its peak, confirming an expansion of the infested areas. In fact, when segment-mean FVC values were averaged across the entire river to examine temporal changes, the maximum average FVC during summer gradually decreased by 9.5% per year during the first three years beginning in 2019, but then reversed sharply and remained at a high level from 2022 onward.

Next, regarding spatial characteristics, St. 1 exhibited a trend in which FVC began to increase around May each year and reached 60–100% in summer, demonstrating stable proliferation of *A. philoxeroides* colonies. A similar trend was observed at St. 2–7 from 2019 to 2022. However, in 2023, FVC at St. 2–4 failed to increase sufficiently. In 2024, FVC at St. 5–7 increased to nearly 100% between March and April but then declined sharply in

May. Meanwhile, at St. 8–12, the maximum summer FVC remained around 50% from 2019 to 2022; however, in 2023, it consistently remained at approximately 60% from April through December, and after a temporary decrease, increased to nearly 100% in May of the following year.

The heatmap shown in Figure 4 contains both observed and interpolated values. Segment-based FVC values derived from Sentinel-2 observations represent the original measurements, whereas values between observation dates and locations were estimated by spatio-temporal Kriging. Because interpolation estimates values between observation dates and river segments, short-term fluctuations and localized changes may be smoothed. Therefore, Figure 4 should be interpreted as a visualization of broad spatio-temporal trends rather than an exact representation of vegetation cover at every time and location. In addition, the downstream expansion discussed in this study was evaluated not only from the interpolated heatmaps but also from the underlying segment-based FVC observations and annual C_{max} patterns.

These results indicate that although localized differences in proliferation status existed among the stations, infestation expansion progressed predominantly downstream across the entire river system, beginning around the summer of 2022.

3.3. Effects of Meteorological Conditions, Removal Operations, and Revetment Types

Using the spatio-temporally estimated segment-mean FVC, the annual maximum fractional vegetation cover (C_{max}) for *A. philoxeroides* was calculated for each year and segment and visualized as a heatmap (Figure 5). Note that because removal operations were conducted from spring to summer in certain segments, C_{max} was not calculated for those years and segments. The spatio-temporal rise and fall of invasive plant colonies are known to be governed not only by species-specific ecological traits but also by environmental factors such as temperature and sunshine duration, river channel conditions such as river geometry and revetment structures, and anthropogenic factors such as the presence or absence of removal operations [28,29]. Therefore, focusing on historical removal records (location and execution date), we examined the relationship between the re-infestation characteristics of *A. philoxeroides* colonies and growth parameters in the Hachiken River.

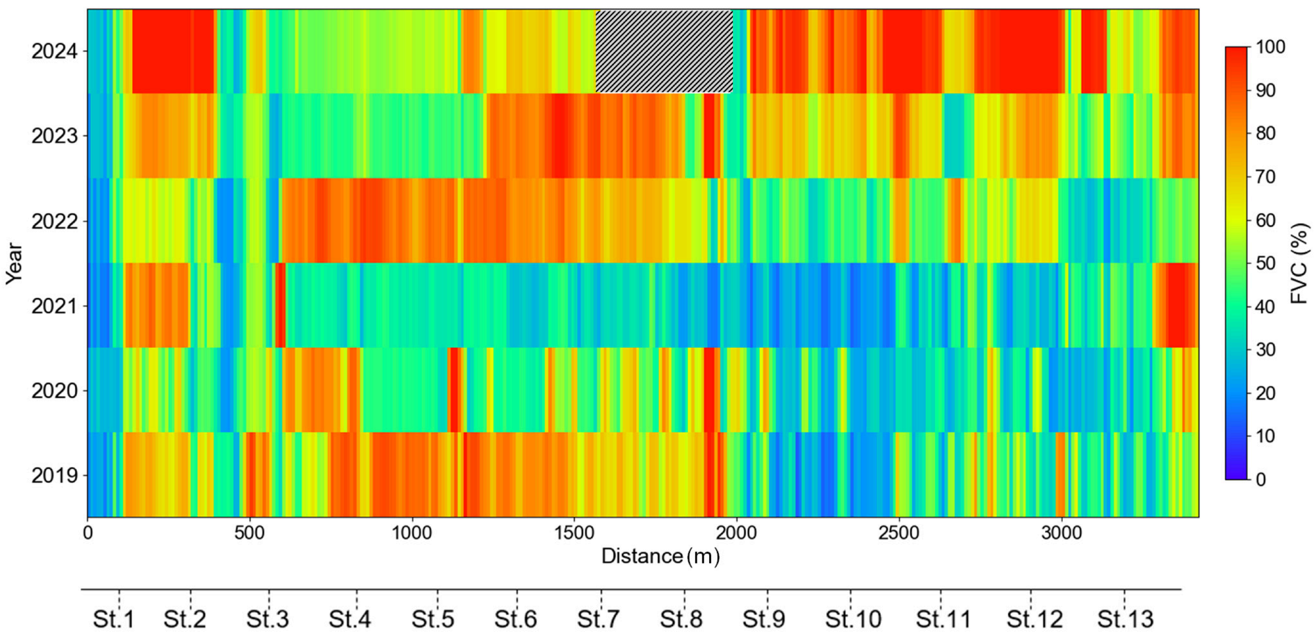

Figure 5. Spatio-temporal heatmap of C_{max} (hatched areas: no data due to it being removed).

3.3.1. Effects of Meteorological Conditions

The establishment and dispersal of invasive plants depend heavily on regional meteorological conditions. Indeed, Pan et al. [30] noted that the physiological activity of this species is maintained within a daily mean temperature range of 10–40 °C, with growth restricted outside this range, and that water flow (precipitation and floods) is a primary driver of plant fragment dispersal. Since flow velocity data were unavailable for the target river, we focused on precipitation data as a potential trigger facilitating the downstream transport of plant fragments.

Table 2 summarizes annual trends in these meteorological conditions during the study period (2019–2024). In this study, the number of days within the aforementioned temperature range was calculated for each year, ranging from 238 to 267 days (mean: 251.5 ± 10.1 days; coefficient of variation [CV] = 4%). This suggests that the growth potential of this species under the prevailing temperature conditions remained largely constant throughout the study period. Furthermore, the analysis of precipitation data showed that annual total precipitation and the number of days with daily precipitation ≥ 30 mm were relatively stable; total precipitation ranged from 1368 to 1982 mm (CV = 14%), and the number of days with precipitation ≥ 30 mm ranged from 11 to 23 (mean: 16.8 ± 3.8 days, CV = 22%), indicating that no extreme events occurred. Annual-scale meteorological indicators showed relatively limited interannual variation during the study period. Therefore, no clear relationship between the observed expansion pattern and the annual meteorological indicators examined in this study was identified. However, the meteorological analysis conducted in this study should be regarded as a preliminary screening based on annual-scale indicators. Although annual temperature and precipitation metrics showed relatively limited variation during the observation period, these indicators may not adequately represent hydrological disturbances that influence the dispersal and establishment of *A. philoxeroides* fragments. Short-term flood events, water-level fluctuations, flow direction, and pumping operations may play a more direct role in invasion dynamics and should be incorporated into future studies when such data become available.

Table 2. Annual variations in temperature and precipitation metrics related to the growth and dispersal of *A. philoxeroides* (2019–2024).

	Days Within the Optimal Temperature Range (Days)	Annual Total Precipitation (mm)	Number of Heavy Rain Days (≥30 mm) (Days)
2019	238	1982	17
2020	249	1580	17
2021	261	1980	18
2022	247	1368	11
2023	267	1526	15
2024	247	1760	23

3.3.2. Efficacy of Removal Operations

According to historical removal records obtained from the river manager, removal operations involving direct mechanical grabbing and extraction of colonies using heavy machinery have been conducted annually in various segments of the downstream reach of the Hachiken River since 2020. Although the target locations varied by fiscal year, approximately 70% of the entire study reach underwent removal at least once. A comparison of the chronological changes in FVC between reaches with and without a history of removal operations showed that reaches subjected to removal generally exhibited lower C_{max} values during the following year, averaging approximately 73% of those observed in reaches without removal operations; however, this difference gradually diminished, and no notable difference was observed by the second year after treatment (Figure 6).

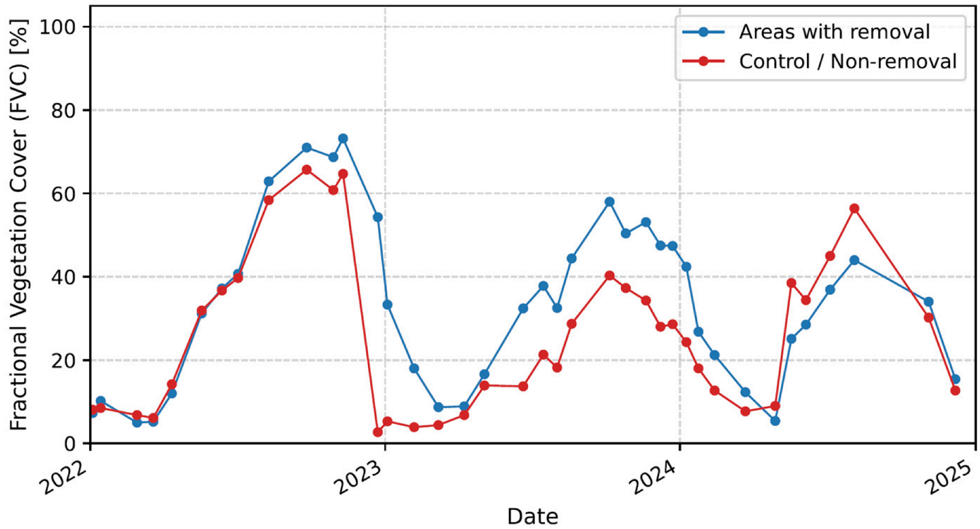

Figure 6. Comparison of FVC between removed and non-removed areas.

This rapid recovery may be associated with a combination of two interconnected factors related to mechanical removal events: "fragment dispersal" and "residual underground biomass." As pointed out by Sainty et al. [31] and Tanveer et al. [32], *A. philoxeroides* possesses an extraordinary capacity for vegetative propagation, where even minuscule stem nodes or rhizome fragments can serve as new sources of establishment. In particular, mechanical extraction with heavy machinery may have inadvertently promoted fragmentation due to intense physical disturbance. According to experiments by Dong et al. [33], isolated nodes of this species exhibit a remarkably high survival rate of 46% on their own, which exceeds 90% when attached to a stem fragment of just a few centimeters. It is inferred that the massive volume of fragments generated by the machinery and left on-site utilized carbohydrates and proteins stored within the internodes as resources [33], enabling rapid re-establishment even in a rootless state and triggering explosive re-infestation. Furthermore, this species has been reported to shift resource allocation to rootstocks in response to aboveground damage [34], which may reinforce underground establishment. Consequently, one possible explanation is that regeneration from residual rhizomes and/or surviving fragments may have contributed to the rapid recovery observed after removal operations. The simultaneous occurrence of regeneration from these residual underground parts and new establishment via fragmentation is considered the primary cause of the rapid re-infestation observed two years after removal.

Meanwhile, around St. 1, which has not undergone any removal since 2022, the year-by-year comparison of FVC temporal dynamics showed that C_{max} rose by an annual average of 19.8%. While C_{max} was reached on 10 November in 2022 and 20 November in 2023, it occurred on 5 July in 2024, shifting 137 days earlier (Figure 7). Dong et al. [33] demonstrated that fragments with longer attached stems and residual leaves exhibit significantly higher growth rates after fragmentation. In unmanaged areas, because extensively interconnected stems and existing leaves are preserved over winter, growth accelerates rapidly in early spring, causing vegetation coverage to reach saturation at a much earlier stage. Additionally, Liu and Yu [35] reported that overwintered mat-like stems can sprout within a single week under favorable environmental conditions, demonstrating rapid regenerative capacity. This suggests that, in unmanaged areas, a prolonged establishment period that allows rhizomes and stems to grow thicker does not merely represent a simple accumulation of biomass, but is highly likely to lead to rapid regeneration in early spring. Although Tanveer et al. [32] reported that global warming and increased precipitation accelerate the distribution expansion and growth rate of this species, regional meteorological data for the study area show no pronounced warming trend during the analysis period. Therefore, while residual rootstocks are currently considered the primary driver, future warming could potentially advance the onset of the growth period itself, leading to even more devastating early-season proliferation through synergistic effects with the surviving underground biomass.

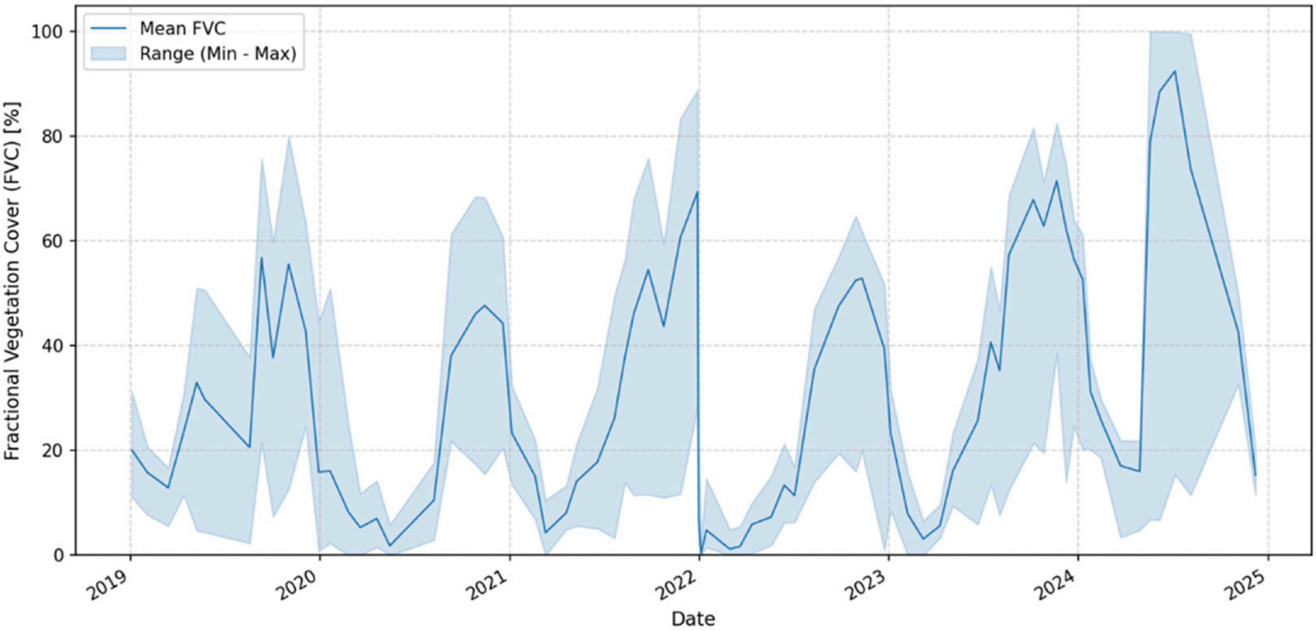

Figure 7. Temporal Changes in Vegetation Cover around St. 1.

The mechanisms discussed above, including regeneration from stem fragments and the survival of residual rhizomes, were not directly examined in this study. Instead, they are presented as possible explanations based on previously reported ecological characteristics of *A. philoxeroides* and the vegetation-cover patterns observed from satellite data. Direct evaluation of fragment production, fragment survival, and belowground persistence would require field-based ecological investigations and remains an important topic for future research.

Although lower C_{max} values were observed in reaches where removal operations had been conducted, this study was based on observational data and did not control for other environmental or management factors. Differences in initial infestation levels, revetment structures, hydrological conditions, management priorities, and spatial connectivity among reaches may also have contributed to the observed patterns. Therefore, the present results should be interpreted as evidence of an association between removal history and subsequent vegetation cover rather than definitive proof of a causal removal effect.

These findings suggest that reaches subjected to removal operations tended to exhibit lower vegetation cover during the following year; however, this difference diminished thereafter, indicating that the observed reduction was not sustained over the longer term. In the medium-to-long term, the population maintains a specific scale while undergoing repeated cycles of re-infestation.

3.3.3. Relationship with Revetment Types

Next, to evaluate the influence of revetment structures on the formation of *A. philoxeroides* colonies, we examined the relationship between C_{max} and revetment type. The study area features a generally linear river geometry, with few topographic depressions where colony fragments would naturally stall and accumulate. On the other hand, multiple types of revetment structures coexist within the reach, and differences in their design and materials may influence the drifting and establishment processes of colony fragments [36]. Due to the spatial resolution constraints of the Sentinel-2 data, this study conducted evaluations using the mean EVI over a 10 m $\times$ river width area, making it impossible to separate the individual influences of the right and left banks. Therefore, the revetment structures were categorized into three types (Type 1: both banks with concrete block revetments; Type 2: one bank with concrete block revetments and one bank with steel sheet piles; Type 3: both banks with steel sheet piles) (Table 3 and Figure 8). The C_{max} values derived from the estimated segment-mean FVC from 2019 to 2024 were then compared among these types.

Table 3. Classification of revetment style (see Figure 8 for images of revetment type).

Type	Revetment Style
1	Both banks: Concrete block
2	One bank: Concrete block, Other bank: Steel sheet pile walls
3	Both banks: Steel sheet pile walls

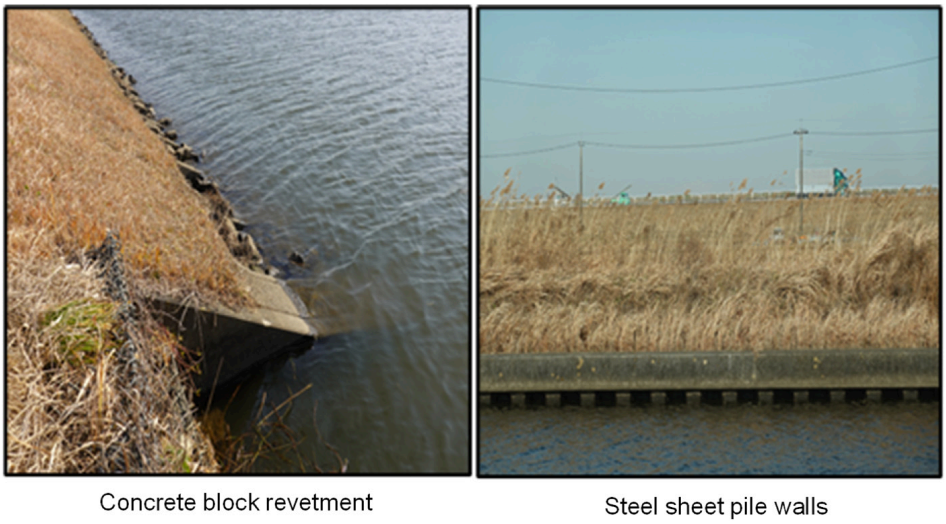

Figure 8. Images of revetment type at Hachiken River.

The results showed that, while Type 1 and Type 2 exhibited similar C_{max} values, Type 3 (both banks with steel sheet piles) suppressed C_{max} to approximately 55% of the levels observed in the other types (Figure 9). C_{max} differed significantly among revetment types (Kruskal–Wallis test, χ^2 = 105.45, df = 2, $p < 2.2 \times 10^{-16}$). Reaches lined with steel sheet piles tended to exhibit lower C_{max} values than reaches with concrete block revetments. This pattern suggests an association between revetment type and colony development; however, the influence of other environmental and management factors cannot be excluded. First, regarding the suppression of initial establishment, steel sheet piles are composed of materials that minimize plant adhesion and penetration [37]. *A. philoxeroides* can regenerate from minute fragments only a few centimeters long and rapidly establish as long as soil is available. In concrete block revetments, joints between blocks and accumulated sediment provide ideal establishment niches for this species. In contrast, steel sheet piles eliminate such physical gaps, preventing drifting fragments from establishing and thereby maintaining low initial population density.

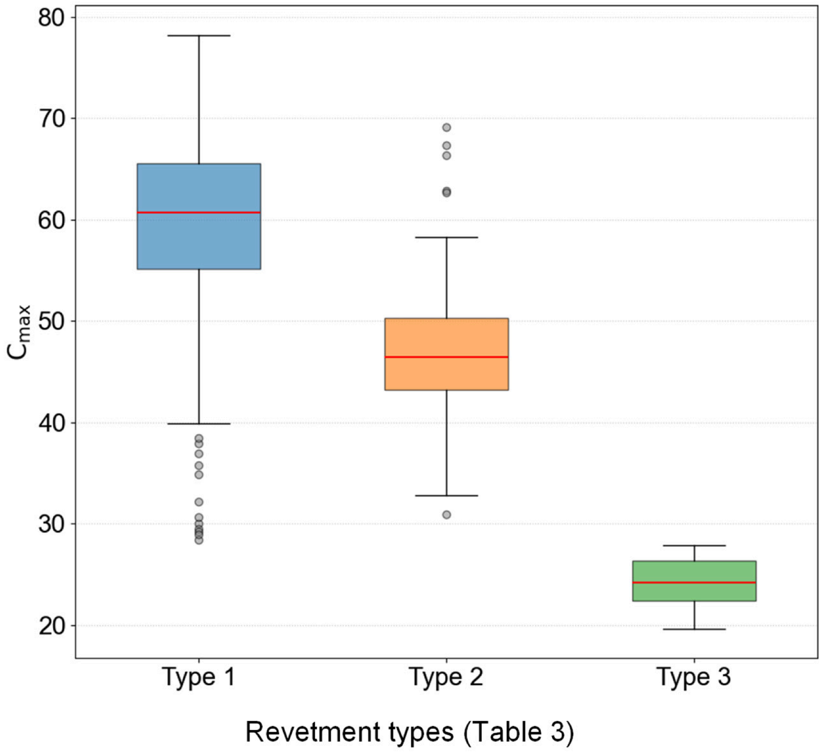

Figure 9. Comparison of C_{max} among revetment types (Table 3).

Second, steel sheet piles may function to block invasion pathways (corridors). Meunier and Lavoie [38] noted that inclined embankment slopes often serve as corridors that facilitate invasion by alien species. Vertical structures such as steel sheet piles physically eliminate these slopes, thereby disrupting continuous expansion from aquatic to terrestrial zones or from upstream to downstream reaches.

Overall, the lower C_{max} values observed in steel-sheet-pile reaches may be associated with a multifaceted combination of environmental and structural factors, including reduced opportunities for establishment, fewer suitable niches, and disruption of invasion corridors over longer time periods. Although revetment type was significantly associated with differences in C_{max}, other environmental and management factors may also have contributed to the observed patterns.

3.4. Scope of Application of the Proposed Method

The spatio-temporal analysis and FVC estimation method based on Sentinel-2 satellite data proposed in this study relies on three primary prerequisites: (1) the river width must encompass at least 2–3 pixels at the spatial resolution of Sentinel-2 (10 m); (2) the flow velocity must be relatively low, providing an environment in which aquatic plant colonies floating on or adhering to the water surface can form stably; and (3) the target reach must be dominated by a single species, or the dominant species must be clearly identifiable.

The proposed framework does not directly identify *A. philoxeroides* from its spectral characteristics. Instead, it estimates vegetation cover under the assumption that *A. philoxeroides* dominates the floating vegetation community within the study reach. Therefore, the approach is most appropriate for river systems where the target species is known to be dominant. In river systems containing substantial mixtures of aquatic plant species, additional field observations or species-classification approaches would be required.

Therefore, this method is particularly suited to capturing relative fluctuations in colony extent within agricultural drainage channels, lowland rivers, and canals where flow dynamics are low and invasive aquatic plants proliferate in linear bands. Conversely, its applicability should be carefully evaluated for mixed-species colonies, torrential rivers subject to frequent flooding, or extremely narrow channels where the river width is less than a single pixel.

4. Conclusions

In this study, we quantitatively evaluated the spatio-temporal dynamics and proliferation characteristics of *A. philoxeroides* colonies in the downstream reach of the Hachiken River using multi-temporal Sentinel-2 satellite data. The results confirmed that, by utilizing EVI, fractional vegetation cover (FVC) could be estimated with an RMSE of 9.2%, even in a narrow river approximately 24 m wide.

Spatio-temporal FVC heatmap analysis integrating river distance and time revealed a trend in which infested areas expanded predominantly in the downstream direction from 2022 onward. Furthermore, comparing annual maximum FVC (C_{max}) with historical removal records and revetment types showed that segments undergoing removal exhibited lower C_{max} values the following year than untreated segments; however, this difference became indistinct by the second year after treatment. Regarding revetment structures, segments with steel sheet piles on both banks consistently maintained lower C_{max} values than those with concrete block revetments, indicating the structural suppression of colony formation. Conversely, in untreated segments, the timing of reaching C_{max} advanced each year, suggesting an increasing risk of severe proliferation under sustained unmanaged conditions.

These findings demonstrate that a relatively simple spatio-temporal analysis framework using Sentinel-2 data can effectively capture the growth characteristics of invasive alien aquatic plant colonies and the impacts of management activities at a river-system scale. The methodology presented in this study remains applicable even in river environments where field surveys or the acquisition of high-resolution data are logistically or financially challenging, and it serves as a foundational framework for the macro-scale evaluation of colony dynamics based on long-term monitoring.

Although the proposed framework was evaluated only within a single 3.5 km narrow, low-flow river reach dominated by *A. philoxeroides*, the results suggest that the approach may be particularly suitable for narrow, slow-flowing waterways dominated by a clearly identifiable aquatic plant species. However, additional validation in river systems with different hydraulic conditions, river widths, and vegetation communities is required before broader application can be assumed.

However, this analysis was conducted under the assumption that *A. philoxeroides* forms a single-species-dominant, floating mat-like colony that broadly covers the water surface within the study reach. Consequently, this method may not be directly applicable to mixed-species colonies, water bodies with complex distributions of submerged or emergent macrophytes, or torrential river environments with frequent flood disturbances. Application of the framework to such environments would require a careful adjustment of index selection and analytical scale.

Future research should build on these wide-area monitoring results by incorporating detailed field surveys to assess precise establishment conditions, along with direct observations of environmental factors such as hydraulic conditions and river channel geometry. This integration will enable a more detailed verification of the physical mechanisms governing the formation and expansion of invasive plant colonies.

https://doi.org/10.3390/rs18152462

5. Patents

A patent application related to the methodology presented in this study has been filed in Japan.

Author Contributions: Conceptualization, K.S.; methodology, K.S.; software, K.S.; validation, K.S.; formal analysis, K.S.; investigation, K.S.; resources, K.S.; data curation, K.S.; writing—original draft preparation, K.S.; writing—review and editing, K.S. and H.K.; visualization, K.S.; supervision, K.S.; project administration, K.S.; funding acquisition, K.S. All authors have read and agreed to the published version of the manuscript.

Funding: This study was funded by the Cabinet Office, Government of Japan, programs for Bridging the gap between R&D and the Ideal society (Society 5.0) and Generating Economic and social value (BRIDGE) (no. R6-09).

Data Availability Statement: The data presented in this study are available on request from the corresponding author due to restrictions imposed by agreements with the river management authority.

Acknowledgments: I would like to thank the Katori Public Office for providing us with the removal data on *A. philoxeroides* and the revetment data for the Hachiken River.

Conflicts of Interest: The authors declare no conflicts of interest.

Abbreviations

The following abbreviations are used in this manuscript:

IAS	Invasive Alien Species
FVC	Fractional Vegetation Cover
NDVI	Normalized Difference Vegetation Index
EVI	Enhanced Vegetation Index
MSAVI	Modified Soil Adjusted Vegetation Index

References

1. Jeschke, J.M.; Bacher, S.; Blackburn, T.M.; Dick, J.T.A.; Essl, F.; Evans, T.; Gaertner, M.; Hulme, P.E.; Kühn, I.; Mrugała, A.; et al. Defining the impact of non-native species. *Conserv. Biol.* **2014**, *28*, 1188–1194. [CrossRef] [PubMed]
2. Seebens, H.; Blackburn, T.M.; Dyer, E.E.; Genovesi, P.; Hulme, P.E.; Jeschke, J.M.; Pagad, S.; Pyšek, P.; Winter, M.; Arianoutsou, M.; et al. No saturation in the accumulation of alien species worldwide. *Nat. Commun.* **2017**, *8*, 14435. [CrossRef] [PubMed]
3. IPBES. *Assessment Report on Invasive Alien Species and Their Control*; Intergovernmental Science-Policy Platform on Biodiversity and Ecosystem Services (IPBES): Bonn, Germany, 2023.
4. Convention on Biological Diversity (CBD). *Strategic Plan for Biodiversity 2011–2020 and the Aichi Biodiversity Targets; Decision X/2*; CBD: Nagoya, Japan, 2010.
5. EPPO Bulletin. Data sheets on pests recommended for regulation: *Alternanthera philoxeroides* (Mart.) Griseb. *EPPO Bull.* **2016**, *46*, 8–13. [CrossRef]
6. Mineta, T.; Sasaki, T.; Ichikawa, Y.; Shibaike, H.; Takahashi, O.; Minakawa, H.; Suzuki, H.; Yamaoka, M. Invading and spreading of *Alternanthera philoxeroides* in the Inbanuma area, Japan. *Water Land Environ. Eng.* **2018**, *86*, 687–690. [CrossRef] [PubMed]
7. The Commonwealth of Australia. *Weeds of National Significance Alligator Weed (Alternanthera philoxeroides) Strategic Plan*; National Weeds Strategy Executive Committee: Launceston, Australia, 2000.
8. Chen, X.; Wang, R.; Cao, Q.; Zhang, H.; Ge, X.; Liu, J. The relationship between the distribution of invasive plant *Alternanthera philoxeroides* and soil properties is scale-dependent. *Pol. J. Environ. Stud.* **2015**, *24*, 1931–1938. [CrossRef] [PubMed]
9. NIES. *Invasive Species of Japan: Alternanthera philoxeroides*; National Institute for Environmental Studies: Tsukuba, Japan, 2026. Available online: https://www.nies.go.jp/biodiversity/invasive/DB/detail/81140e.html (accessed on 1 April 2026).
10. Kim, C.S.; Lubowski, R.N.; Lewandrowski, J.; Eiswerth, M.E. Prevention or control: Optimal government policies for invasive species management. *Agric. Resour. Econ. Rev.* **2006**, *35*, 29–40. [CrossRef]
11. Mehta, S.V.; Haight, R.G.; Homans, F.R.; Polasky, S.; Venette, R.C. Optimal detection and control strategies for invasive species management. *Ecol. Econ.* **2007**, *61*, 237–245. [CrossRef]

12. Ramula, S.; Knight, T.M.; Burns, J.H.; Buckley, Y.M. General guidelines for invasive plant management based on comparative demography of invasive and native plant populations. *J. Appl. Ecol.* **2008**, *45*, 1124–1133. [CrossRef]
13. Santos, M.J.; Anderson, L.W.; Ustin, S.L. Effects of invasive species on plant communities: An example using submersed aquatic plants at the regional scale. *Biol. Invasions* **2011**, *13*, 443–457. [CrossRef]
14. Glenn, E.; Tanner, R.; Mendez, S.; Kehret, T.; Moore, D.; Garcia, J.; Valdes, C. Growth rates, salt tolerance and water use characteristics of native and invasive riparian plants from the delta of the Colorado River, Mexico. *J. Arid. Environ.* **1998**, *40*, 281–294. [CrossRef]
15. Hama, T.; Hamada, S.; Kondo, A. Exotic aquatic plants monitoring by multi-temporal proximity aerial photos in Kannou River, Inbanuma catchment, Chiba, Japan. In *Proceedings of the General Meeting of the Association of Japanese Geographers*; The Association of Japanese Geographers: Tokyo, Japan, 2016; p. 100132. [CrossRef] [PubMed]
16. Evrendilek, F.; Gulbeyaz, O. Deriving vegetation dynamics of natural terrestrial ecosystems from MODIS NDVI/EVI data over Turkey. *Sensors* **2008**, *8*, 5270–5302. [CrossRef] [PubMed]
17. Jakubauskas, M.E.; Peterson, D.L.; Campbell, S.W.; deNoyelles, F.; Campbell, S.D.; Penny, D. Mapping and monitoring invasive aquatic plant obstructions in navigable waterways using satellite multispectral imagery. In Proceedings of the Pecora 15/Land Satellite Information IV Conference, Denver, CO, USA, 10–15 November 2002; pp. 20–24.
18. Müllerová, J.; Pergl, J.; Pyšek, P. Remote sensing as a tool for monitoring plant invasions: Testing the effects of data resolution and image classification approach on the detection of a model plant species Heracleum mantegazzianum (giant hogweed). *Int. J. Appl. Earth Obs. Geoinf.* **2013**, *25*, 55–65. [CrossRef]
19. Clements, D.; Dugdale, T.M.; Hunt, T.D. Growth of aquatic alligator weed (*Alternanthera philoxeroides*) over 5 years in south-east Australia. *Aquat. Invasions* **2011**, *6*, 77–82. [CrossRef]
20. Buckingham, G.R. Biological control of alligatorweed, *Alternanthera philoxeroides*, the world's first aquatic weed success story. *Castanea* **1996**, *61*, 232–243.
21. Huang, C.; Asner, G.P. Applications of remote sensing to alien invasive plant studies. *Sensors* **2009**, *9*, 4869–4889. [CrossRef] [PubMed]
22. Sheffield, K.J.; Clements, D.; Clune, D.J.; Constantine, A.; Dugdale, T.M. Detection of aquatic alligator weed (*Alternanthera philoxeroides*) from aerial imagery using random forest classification. *Remote Sens.* **2022**, *14*, 2674. [CrossRef]
23. Huete, A.; Justice, C.; Liu, H. Development of vegetation and soil indices for MODIS-EOS. *Remote Sens. Environ.* **1994**, *49*, 224–234. [CrossRef]
24. Duncan, P.; Podest, E.; Esler, K.J.; Geerts, S.; Lyons, C. Mapping invasive herbaceous plant species with Sentinel-2 satellite imagery: *Echium plantagineum* in a Mediterranean Shrubland as a Case Study. *Geomatics* **2023**, *3*, 328–344. [CrossRef]
25. Verschoren, V.; Schoelynck, J.; Buis, K.; Visser, F.; Meire, P.; Temmerman, S. Mapping the spatio-temporal distribution of key vegetation cover properties in lowland river reaches, using digital photography. *Environ. Monit. Assess.* **2017**, *189*, 294. [CrossRef] [PubMed]
26. Liu, C.; Zhang, X.; Wang, T.; Chen, G.; Zhu, K.; Wang, Q.; Wang, J. Detection of vegetation coverage changes in the Yellow River Basin from 2003 to 2020. *Ecol. Indic.* **2022**, *138*, 108818. [CrossRef]
27. Iwasa, Y. *Suri-Seibutugaku Nyuumon*; Kyoritsu Shuppan: Tokyo, Japan, 1990. [CrossRef]
28. Kusumoto, Y.; Tokuoka, Y.; Yamamoto, S. Distributional expansion factors of *Alternanthera philoxeroides* in paddy fields of Inba-numa Area, Japan. *J. Rural Plan. Assoc.* **2011**, *30*, 249–254. [CrossRef]
29. Minagawa, T.; Uesugi, K.; Ito, R. Distribution and habitat of *Alternanthera philoxeroides*, a Invasive Alien Species in the Kikuchi River. *J. Jpn. Soc. Civ. Eng. Ser. B1 (Hydraul. Eng.)* **2021**, *77*, I_1039–I_1044. [CrossRef] [PubMed]
30. Pan, X.Y.; Geng, Y.P.; Sosa, A.; Zhang, W.J.; Li, B.; Chen, J.K. Invasive *Alternanthera philoxeroides*: Biology, ecology and management. *Acta Phytotaxon. Sin.* **2007**, *45*, 884–900. [CrossRef]
31. Sainty, G.; McCorkelle, G.; Julien, M. Control and spread of Alligator Weed, *Alternanthera philoxeroides* (Mart.) Griseb., in Australia: Lessons for other regions. *Wetl. Ecol. Manag.* **1997**, *5*, 195–201. [CrossRef]
32. Tanveer, A.; Ali, H.H.; Manalil, S.; Raza, A.; Chauhan, B.S. Eco-biology and management of alligator weed [*Alternanthera philoxeroides*) (Mart.) Griseb.]: A Review. *Wetlands* **2018**, *38*, 1067–1079. [CrossRef]
33. Dong, B.C.; Yu, G.L.; Guo, W.; Zhang, M.X.; Dong, M.; Yu, F.H. How internode length, position and presence of leaves affect survival and growth of *Alternanthera philoxeroides* after fragmentation? *Evol. Ecol.* **2010**, *24*, 1447–1461. [CrossRef]
34. Sun, Y.; Ding, J.; Frye, M.J. Effects of resource availability on tolerance of herbivory in the invasive *Alternanthera philoxeroides* and the native *Alternanthera sessilis*. *Weed Res.* **2010**, *50*, 527–536. [CrossRef]
35. Liu, C.; Yu, D. The bud and root sprouting capacity of *Alternanthera philoxeroides* after over-wintering on sediments of a drained canal. *Hydrobiologia* **2009**, *623*, 251–256. [CrossRef]
36. Oki, Y. How to deal intelligently with the management of alien aquatic plants. *Jpn. J. Limnol.* **2009**, *70*, 255–260. [CrossRef]

37. Tsuchiya, M.; Izumi, K. A study for statement of river environment. *Annu. J. Hydraul. Eng.* **1990**, *34*, 55–60. [CrossRef]
38. Meunier, G.; Lavoie, C. Roads as corridors for invasive plant species: New Evidence from Smooth Bedstraw (*Galium mollugo*). *Invasive Plant Sci. Manag.* **2012**, *5*, 92–100. [CrossRef]

https://doi.org/10.3390/rs18152462